

Studying of 1-D assemblies in anionic azo dyes and cationic surfactants mixed systems

Xin-hao Cheng, Yu Peng, Chen Gao, Yun Yan*, Jian-bin Huang*

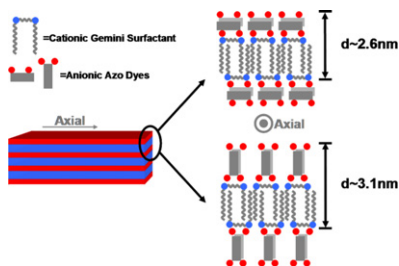
Beijing National Laboratory for Molecular Sciences (BNLMS) (State Key Laboratory for Structural Chemistry of Unstable and Stable Species), College of Chemistry and Molecular Engineering, Peking University, Beijing 100871, PR China

HIGHLIGHTS

- ▶ 1-D structures were found in azo dyes and cationic surfactants mixed systems.
- ▶ Helixes were found in one of the mixed systems.
- ▶ The regulation of the formation of these 1-D structures has been investigated.

GRAPHICAL ABSTRACT

Combination of steric effect, π - π stacking, electrostatic and hydrophobic interaction, the packing model of dye and surfactant molecules in the 1-D nano-structures has been suggested.



ARTICLE INFO

Article history:

Received 12 November 2012
 Received in revised form
 17 December 2012
 Accepted 20 December 2012
 Available online xxx

Keywords:

One-dimensional
 Self-assembly
 Gemini surfactants
 Azo dyes

ABSTRACT

The construction and regulation of one-dimensional (1-D) structure have been fully investigated in anionic azo dyes and cationic surfactants mixed systems. Anionic azo dyes with different charge numbers and different size of conjugated groups were selected. Analogously, cationic alkyl quaternary ammoniums surfactants with different chain length, charges on the head, and types of the surfactants were tested. By studying the relationship between molecular structure and intermolecular interactions in a controlled way, it was found that 1-D self-assembly is a process that affected by multiple interactions, including electrostatic attractions, hydrophobic interactions, and potential π - π staking. Besides, the symmetry of the molecules also affects the morphology of the assemblies.

© 2013 Elsevier B.V. All rights reserved.

1. Introduction

Recently, one-dimensional (1-D) nano-structures have received an intensive attention owing to their superior electronic [1–6], optical [7–9], sensing [10–12], and energetic [13] properties resulted from the quantum-confinement effects and high surface area to volume ratio, and are expected to be applied in biological sensing

* Corresponding authors. Tel.: +86 10 62765058; fax: +86 10 62765058.
 E-mail addresses: yunyan@pku.edu.cn (Y. Yan), jbhuang@pku.edu.cn (J.-b. Huang).

[14] and disease diagnoses [15–18]. So far, many attempts have been made to achieve 1-D nano-structures such as vapor deposition [19], solution–liquid–solid method [20], template-directed methods [21–24], and molecular self-assembly [25–30]. Among these, self-assembly in aqueous solution is a simple and mild way to construct 1-D nano-structures since it allows rational control of the shape and size of 1-D nano-structures. Combining the non-directional interactions such as electrostatics, solvophobicity, directional forces such as coordination binding, hydrogen bonding, and π - π stacking, via molecular design, one may obtain, well-defined 1-D structures with different properties [31]. Typical examples are 1-D nano-structures assembled from conjugated

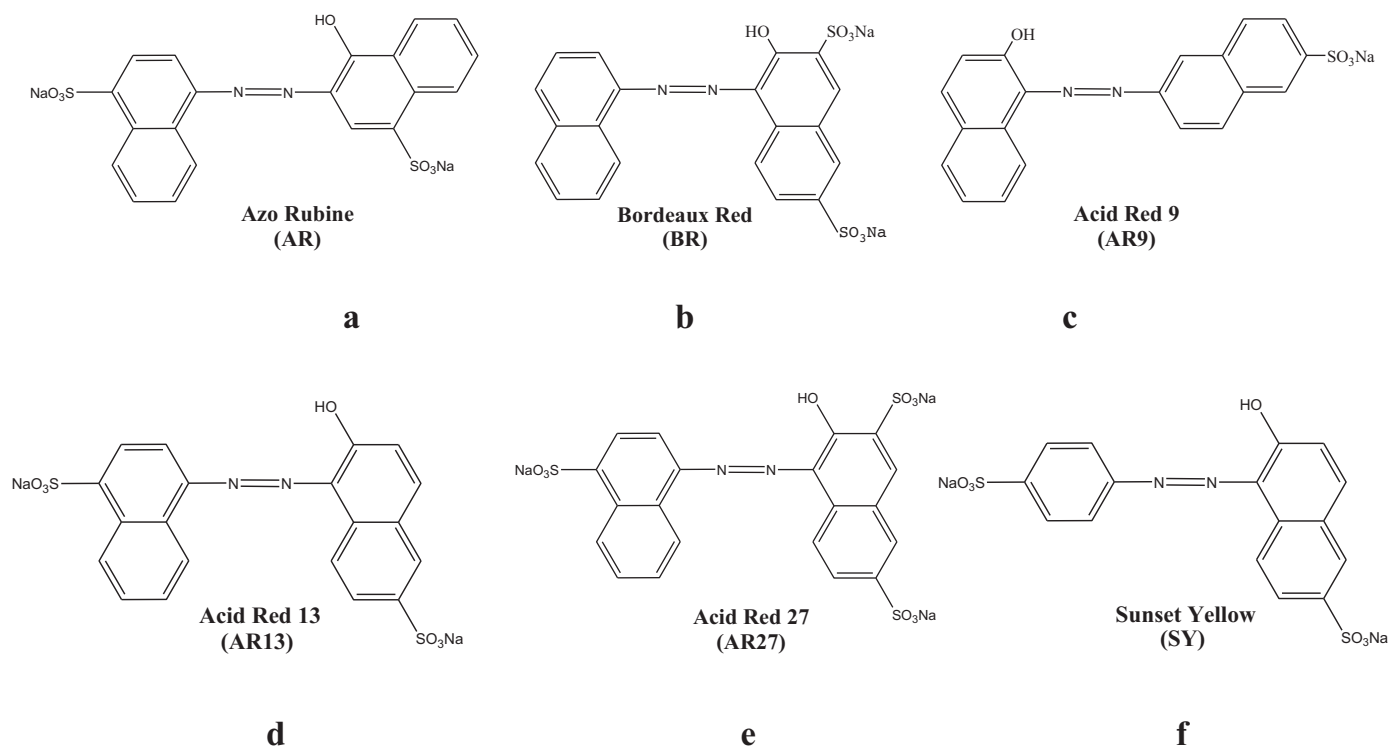


Fig. 1. Schemes of chemical structure of azo-dyes.

disk-like molecules or dyes, where the symmetry and π - π interactions among the conjugated groups define the orientation of 1-D self-assembly. For example, Shelnut reported the formation of nano-fibers by two oppositely charged porphyrins in aqueous solution [32]. Faul studied the formation of nanotubes by two oppositely charged dyes with different frame structure (porphyrins and perylenes) [33]. Besides, dyes (often carrying negative charges) were also co-assembled with surfactants or other molecules via electrostatic interaction, hydrogen bonding and coordination interaction to construct 1-D nano-structures. For instance, Burger achieved ribbon-like aggregates by perylenetetracarboxylic dianhydride, which has a negative charged perylene frame structure and optical ionic of quaternary ammonium with two hydrophobic chains [34]. Similarly, Hoffmann reported the formation of nano-fibers in the mixed systems of dyes and surfactants, where the morphology of the fibers was controlled by the mixed ratio [35]. Fine-tune of the 1-D self-assembled structures were achieved by Faul and co-workers, through introduction of the hydrogen bonding [36], coordinating [37], and chiral centers into the surfactants [38]. In our recent studies, nano-fibers were constructed in different systems, including the mixed system of an aromatic anionic surfactant and oppositely charged aromatic hydrotropic salt [26], the mixed system of negative charged bile salts and various metal ions [30], and azo-modified surfactants with head groups of dipeptide [27] and glycosylamine [28]. The driving forces in these systems are including electrostatic attraction, hydrophobic interactions, π - π interactions, coordination interactions and hydrogen bonds.

In spite of the elegant studies on the aforementioned 1-D nano-structures based on dyes, the role of non-covalent interactions that participate in the assembling process is still lack of systematic study. This work aims to establish the relation between the molecule structure and the morphology of the self-assemblies, and to understand the role of non-covalent interactions on the formation of 1-D self-assembly. To this end, 1-D assemblies formed in a series of mixed systems of azo dyes and surfactants were

studied. The dyes have similar structures (Fig. 1) which differ either in charge numbers, or in the size of aromatic rings. Analogously, the structure of the cationic surfactant was also varied in a rationally controlled way, including changing the chain length, the charges on the head, as well as varying the type of the surfactants, namely from classical to Gemini with spacers of various length. Upon considering these structural factors one by one, we are able to obtain a systematic knowledge about the role of head group sizes, charge density matching, π - π interactions, and hydrophobic interactions on the 1-D structure formation.

2. Materials and methods

2.1. Materials

Acid Red 13 (AR13), Acid Red 27 (AR27), Azo Rubine (AR), Sunset Yellow (SY), Acid Red 9 (AR9) and methyl orange (MO) were purchased from TCI. Bordeaux Red (BR) was from Acros Organics Co. Dodecyltrimethylammonium bromide (DTAB), sodium dodecylsulfate (SDS) and *p*-octyl polyethylene glycol phenyl ether (Triton X-100) were from Alfa Aesar. All these chemicals were used as received. Quaternary ammonium bromides were prepared by reaction of 1-bromododecane and the corresponding trialkylamine as described in our previous paper. The abbreviations of the quaternary ammonium bromides are listed as follows: dodecyltriethylammonium bromide (DEAB); dodecyltripropylammonium bromide (DPAB); octyltributylammonium bromide (OTAB); decyltributylammonium bromide (DeTAB); dodecylpyridinium bromide (DPyB) and dodecylmethylimidazolium bromide (DMIImB). The Gemini surfactants alkylene-*a,s*-bis(dodecyldimethylammonium bromide) (12-*s*-12(Me)) (*s* = 4, 6, 10) were synthesized in this lab according to the procedure reported elsewhere [39]. Milli Q water was used throughout this work. All other reagents were products of A.R. grade.

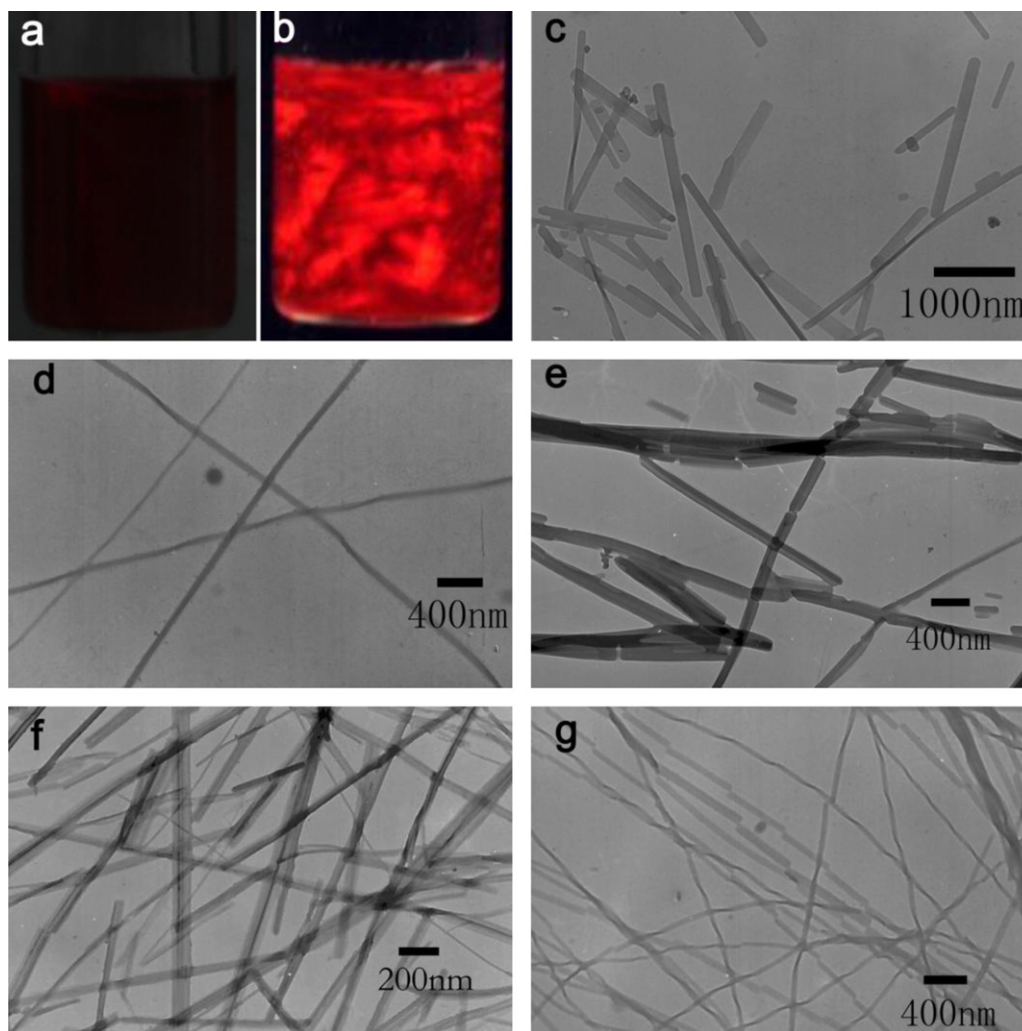


Fig. 2. (a) Fresh mixture of AR/12-6-12(Me), under polarizer; (b) after two days, under polarizer; (c) TEM image of AR9/12-6-12(Me) charge ratio = 1:1 system, $C_T = 1$ mM; (d) TEM image of AR13/12-6-12(Me) charge ratio = 1:2 system, $C_T = 1$ mM; (e) TEM image of AR27/12-6-12(Me) charge ratio = 2:1 system, $C_T = 1$ mM; (f) TEM image of BR/12-6-12(Me) charge ratio = 2.5:1 system, $C_T = 3$ mM; (g) TEM image of AR/12-6-12(Me) charge ratio = 1:1 system, $C_T = 1$ mM.

2.2. Sample preparation

Samples were prepared by mixing aqueous solutions of surfactant and dye at certain mixing ratio. These samples were vortex mixed and were maintained at 25 °C in a thermostatic bath at least for three days before measurements.

2.3. Transmission electron microscopy (TEM)

Micrographs were obtained with a JEM-100CX II transmission electron microscope. For negative-stained samples, uranyl acetate solution (1%) was used as the staining agent. One drop of the samples was placed onto a carbon Formvar-coated copper grid (230 mesh), and the excess water was removed with a piece of filter paper. Then a drop of staining agent was placed to the grid loading samples. After a couple of seconds, the excess staining agent was removed with filter paper again.

2.4. Dynamic light scattering measurements (DLS)

DLS were carried out using a spectrometer of standard design (ALV-5000/E/WIN Multiple Tau Digital Correlator) with a 22 mW Ar laser (wavelength: 632.8 nm). The temperature was controlled at 25 ± 0.5 °C using a Haake C35 thermostat. To prepare dust-free

solutions for light scattering measurements, the solutions were filtered through a 0.22 μm membrane of hydrophilic PVDF filter into light scattering cells before the measurements. The scattering angle was 90°.

2.5. X-ray diffraction (XRD)

For XRD measurements, several drops of the suspension were dropped on a clean glass slide, followed by drying in air. Reflection XRD studies were carried out for the film with a model XKS-2000 X-ray diffractometer (Scintaginc). The X-ray beam was generated with a Cu anode, and the wavelength of the $K_{\alpha 1}$ beam was 1.5406 Å. The X-ray beam was directed toward the film edge, and the scanning was done up to a 2θ range from 2 to 10° and 2 to 30°.

3. Results and discussion

3.1. Assemblies in the mixed systems of dyes and Gemini surfactant 12-6-12(Me)

We first studied the mixed solutions of azo dyes (including AR, AR9, AR13, AR27, BR) with a Gemini surfactant hexylene-1,6-bis(dodecyldimethylammonium bromide) (12-6-12(Me)). All the fresh aqueous mixtures of azo dyes and Gemini surfactants are

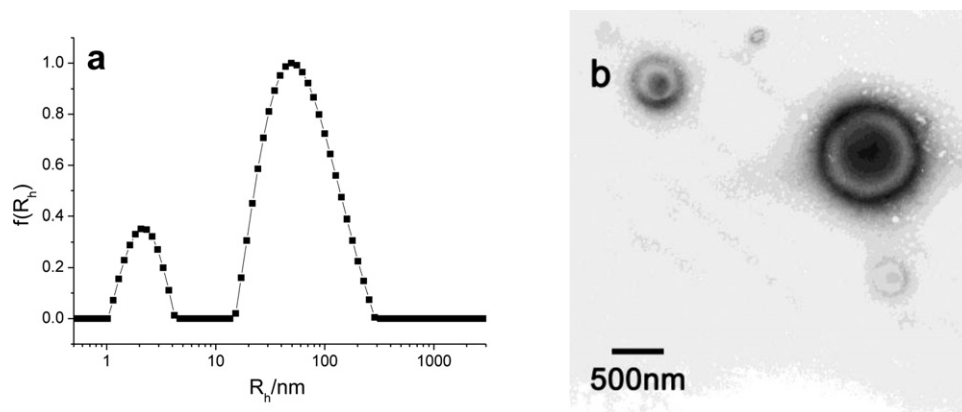


Fig. 3. (a) Size distribution and (b) TEM image of AR/12-6-12(Me) charge ratio = 1:9 $C_T = 1$ mM system.

transparent homogeneous solution at 25 °C (Fig. 2a). Two days later, a strong birefringence phenomenon can be observed (Fig. 2b), which suggests the formation of unsymmetrical structures in these solutions.

If we define the molar fraction of the dyes in azo dyes and Gemini surfactants mixed systems as $r = n_{\text{dye}} / (n_{\text{dye}} + n_{\text{surfactant}})$, it was found that the 1-D nano-structures can be observed in a wide range of r at various concentrations. Although precipitation was formed in all of the mixtures at the total concentration beyond 0.005 mM and r beyond 0.1, the microstructures can be analyzed by using TEM. For the corresponding AR and AR9 mixed systems, TEM results revealed that the precipitates are formed solely by 1-D nano-structures as well. However, for the AR13/12-6-12(Me) mixed system, nano-fibers were observed in a limit range of $0.1 < r < 0.5$, whereas random precipitates were found at other ratios. Similar phenomena occurred to the AR27/12-6-12(Me) and BR/12-6-12(Me) mixed systems: nano-fibers were formed at $0.5 < r < 1$. TEM results revealed that 1-D nano-structures of 10–200 nm width can be observed in the birefringent solutions (Fig. 2c–g). In AR9/12-6-12(Me) and AR27/12-6-12(Me) systems, the nano-structures are rigid and run up to several micrometers. In AR/12-6-12(Me), AR13/12-6-12(Me) and BR/12-6-12(Me) systems, the nano-structures are soft and fiber-like, which can be hundreds micrometers or even longer. It can be clearly visualized that the aggregates in AR/12-6-12(Me) system are a mixture of nano-fibers and nano-helices (Fig. 2g).

At r below 0.1, no precipitates can be observed in all of the five dye/surfactant systems. DLS results suggest the presence of two families of particles with the hydrodynamic radius R_h around 2 nm and 50 nm, respectively. TEM observation verified the larger ones are vesicles, whereas the smaller ones can be attributed to micelles which are invisible under TEM. The vesicles in the five mixed systems of various dyes and 12-6-12(Me) are all with radius being 50–200 nm under TEM. (Fig. 3) The phase diagrams of the dyes/12-6-12(Me) systems are showed in Fig. 4.

These 1-D nano-structures are stable between 0 °C and 55 °C. However, at temperature higher than 55 °C, they shrink into random precipitates in a few minutes and the process is irreversible.

The formation rate of these 1-D nano-structures is closely related with temperature, concentration, and r . First of all, the rate of formation is fast at high temperature. For instance, the nano-fibers in the AR/12-6-12(Me) 1:1 system ($C_T = 1$ mM) will form within hours and reach equilibrium in one or two days at 25 °C, while it takes several weeks to arrive at stable state at 4 °C. Secondly, it is very interesting to find a negative correlation between the concentration and the rate of 1-D nano-structure formation, namely, the higher the concentration is, the slower the

nano-structures form. For instance, the nano-fibers start to occur in 2 h at 25 °C in $C_T = 1$ mM system (Fig. 5a) and grow beyond one hundred micrometers within one day (Fig. 5b), which morphology have little change contrasting with that of 48 h (Fig. 5c). In contrast, it takes two days to reach the corresponding stage in the 5 mM system, (Fig. 5e). Thirdly, r also affects the rate of formation for these 1-D structures. For example, it takes one day for the 1-D nano-structures in the AR/12-6-12(Me) system ($C_T = 1$ mM, 25 °C) to reach equilibrium if $r < 0.67$ ($n_{\text{AR}}/n_{12-6-12(\text{Me})} < 2/1$). In contrast, the equilibrium may be completed immediately at $r \geq 0.67$.

3.2. The effect of surfactant types

In order to get a general rule on the 1-D structure formation, further experiments are performed in mixed systems of AR and different types of surfactants. First of all, we compared the structural difference of conventional surfactants and Geminis. It is well known that Geminis usually exhibit stronger aggregation ability and have more versatility in aggregate morphology than the conventional ones of the same chain length. Therefore, we hope to clarify whether it is the special Gemini structure that triggered the 1-D structure formation. For this purpose, self-assembly formed in the mixed systems of azo dyes and conventional surfactant DTAB, which has the same chain length with 12-6-12(Me) were examined. It was found that the assemblies in the mixed systems of azo dyes with conventional surfactants are also one dimensional, except that they are broader. For instance, in the AR9/DTAB, BR/DTAB, and AR27/DTAB systems, the assemblies are all ribbon-like or plate-like with widths over 1 μm . In the AR/DTAB and AR13/DTAB systems, the assemblies are still fiber-like only that their widths are increased. The major difference is that there are no helices in the AR/DTAB systems. Comparing the XRD results of dyes/Gemini surfactants and those of dyes/conventional surfactants, it is found that dyes/conventional surfactants have much sharper peaks, which stands for better crystallinity.

3.3. The effect of electrostatic interactions

The above results suggest that the Gemini structure is not the determinative role for the 1-D structure formation; it seems that the interaction between the surfactant and the dyes are very crucial. In order to analyze the role of electrostatic interaction among the interactions, we use conventional surfactants with various head groups to make further systematic studies in case of necessary. In Table 1 we list the structures formed by dyes with surfactants with various electrical states.

Table 1 clearly demonstrates that neither nonionic nor anionic surfactant systems are able to form 1-D structures. In contrast, if

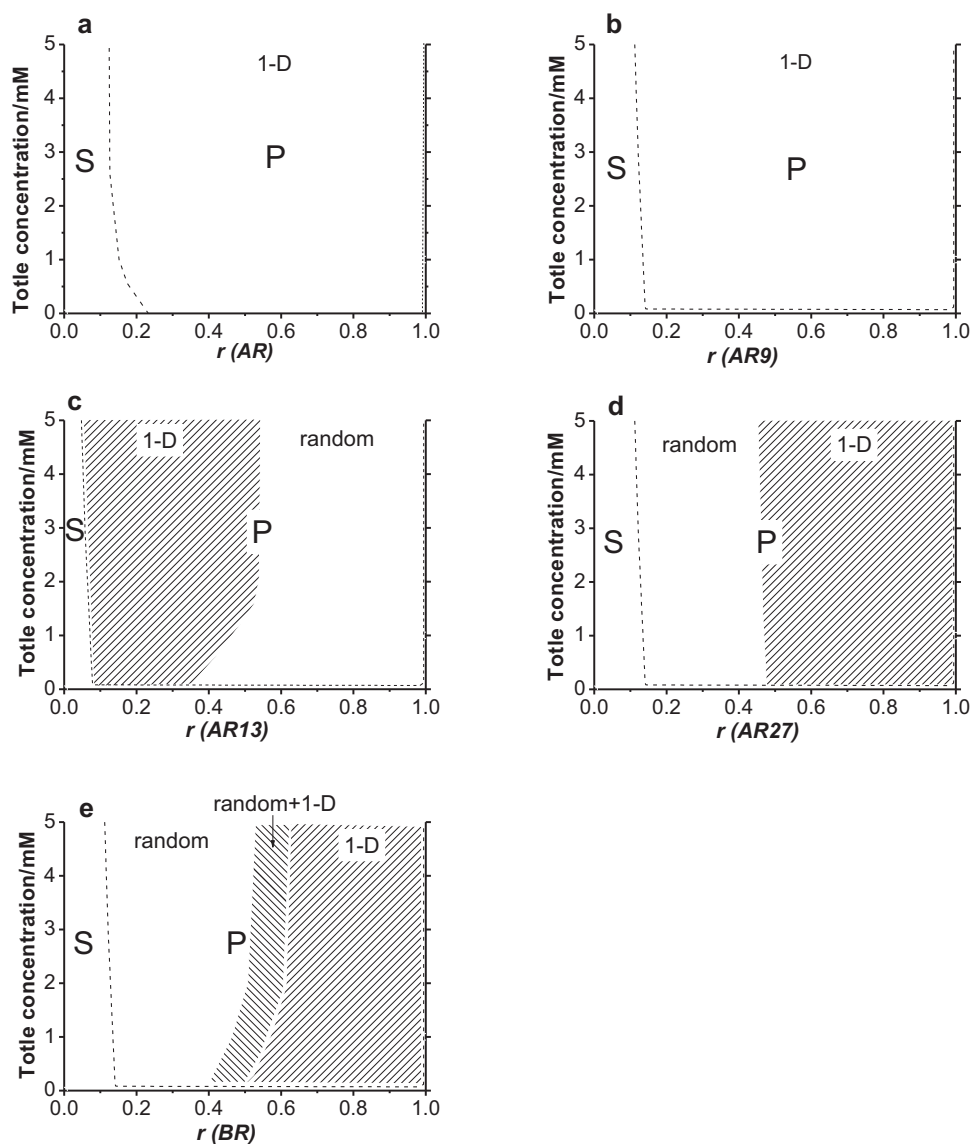


Fig. 4. Phase diagrams of the dyes/12-6-12(Me) systems at 25 °C: (a) AR/12-6-12(Me); (b) AR9/12-6-12(Me); (c) AR13/12-6-12(Me); (d) AR27/12-6-12(Me); (e) BR/12-6-12(Me). S stands for solution, while P stands for precipitation.

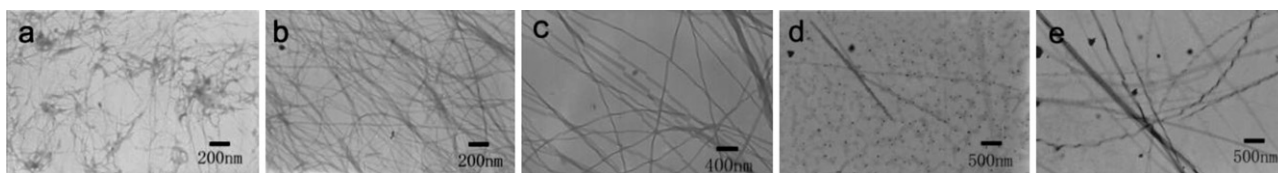


Fig. 5. TEM images of AR/12-6-12(Me) charge ratio = 1:1 systems at 25 °C: (a) $C_T = 1$ mM, 2 h; (b) $C_T = 1$ mM, 24 h; (c) $C_T = 1$ mM, 48 h; (d) $C_T = 5$ mM, 24 h; (e) $C_T = 5$ mM, 48 h.

Table 1

The aggregation states of AR/Surfactant (of different electrical state) complex.

Surfactant	Aggregates
Triton X-100	no self-assemblies observed
SDS	no self-assemblies observed
DTAB	nano-fibers
12-6-12(Me)	nano-fibers and nano-helices (Fig. 2g)

cationic surfactants were employed, either conventional or Gemini type, 1-D nano-structures are always observed by TEM. Apparently, the electrostatic attraction between anionic dyes and opposite charged surfactants is essential to the formation of nano-structure.

3.4. The effect of the structure of azo dyes

Although electrostatic attraction is proved to be a key driving force, directional interaction, such as π - π Staking, is also necessary for the formation of the 1-D structure. To unravel such an effect, self-assemblies were compared in dyes of various structures with 12-6-12(Me).

It is clear from Table 2 that the number of charges on the azo dyes (AR9, AR13, AR27) and the frame structure (AR13, AR) does not influence the formation of 1-D nano-structures. However, when the size of conjugate groups decreased, 1-D nano-structures cannot be observed anymore. With further decreasing the size of the

Table 2
The aggregation states of azo dyes/12-6-12(Me) complex.

Azo dye	Aggregates
AR	nano-fibers and nano helixes (Fig. 2g)
AR9	nano-rods (Fig. 2c)
AR13	nano-fibers (Fig. 2d)
AR27	nano-rods (Fig. 2e)
BR	nano-fibers (Fig. 2f)
SY	block
MO	no self-assemblies were observed

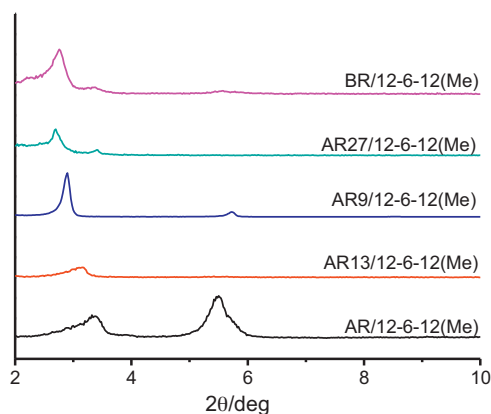


Fig. 6. X-Ray diffraction result of the dye/surfactant systems.

conjugate groups (Methly Orange, MO), transparent solution is formed instead of precipitation, which indicates a decrease in the interaction among dyes and surfactants. This suggests that π - π interaction in the mixed systems may play a key role in the formation of 1-D nano-structures besides electrostatic attraction.

Interestingly, XRD results suggest that these dyes may have different packing modes. The peaks of 2θ around 2.7–3.4 degrees correspond to distances between 3.3 and 2.6 nm. (Fig. 6) These peaks can be divided into two groups. The complexes of AR9, AR27 and BR with 12-6-12(Me) have a repeat unit over 3 nm (AR9/12-6-12(Me): 3.04 nm; AR27/12-6-12(Me): 3.27 nm; BR/12-6-12(Me):

3.20 nm.), while AR and AR13 have a repeat unit of 2.61 nm and 2.79 nm respectively. It is worth mention that the AR27 and BR also have small peaks of 2θ around 3.4 degrees, which are corresponded to a repeat unit of 2.60 nm. According to Faul's study of a similar system, these peaks can be attributed to the lamellar structure of spaced dyes and surfactants [40]. It is noticeable that the charges on AR9, BR, and AR27 are located in the same naphthalene ring, while the charges of AR and AR13 are separated in different naphthalene rings. This different charge distribution on the dyes is probably the crucial role that determines the molecular packing in the self-assemblies. It is well-known that the π - π interaction may lead to the 1-D orientation [31]. In our study, this may also occur between the dye molecules. Taking into account the hydrophobic interactions contributed by the surfactant chains which tend to assemble to minimize the contact with water, a possible model of the assemblies is suggested (Fig. 7). In this model, the rigid dye scaffolds are in an anti-parallel arrangement forming the crystalline layers with the alkyl chains alternating into the two neighboring alkyl layers. The potential π - π stacking between the dye molecules tends to be perpendicular to the axis of the nano-fibers, which makes the assemblies favor one-dimensional growth, rather than formation of two-dimensional plane. The long axis of AR9, AR27 and BR is mainly parallel to the hydrophobic chains, so that the overall length of the electrostatic complexes, which is the repeating unit in the self-assembled structures, is ~ 3.1 nm. In contrast, the long axis of AR and AR13 is perpendicular to the hydrophobic chains, which results in an overall length for the electrostatic complexes being ~ 2.6 nm. It should be pointed out that in AR27/12-6-12(Me) and BR/12-6-12(Me) systems, a few nano-structures also have a molecular arrangement with the dyes' long axis perpendicular to the hydrophobic chains, but they are not dominant conformation.

3.5. The effect of the surfactants' structure

The size of the head group of the surfactants also influences the formation of 1-D nano-structure in these mixed systems. (Table 3) For surfactants with chain length of 12 carbons, 1-D structures can be formed when the head groups are amine hydrochloride (DDHC) and trimethyl ammonium (DTAB) in the mixture with various azo dyes. However, when the head groups were replaced by larger

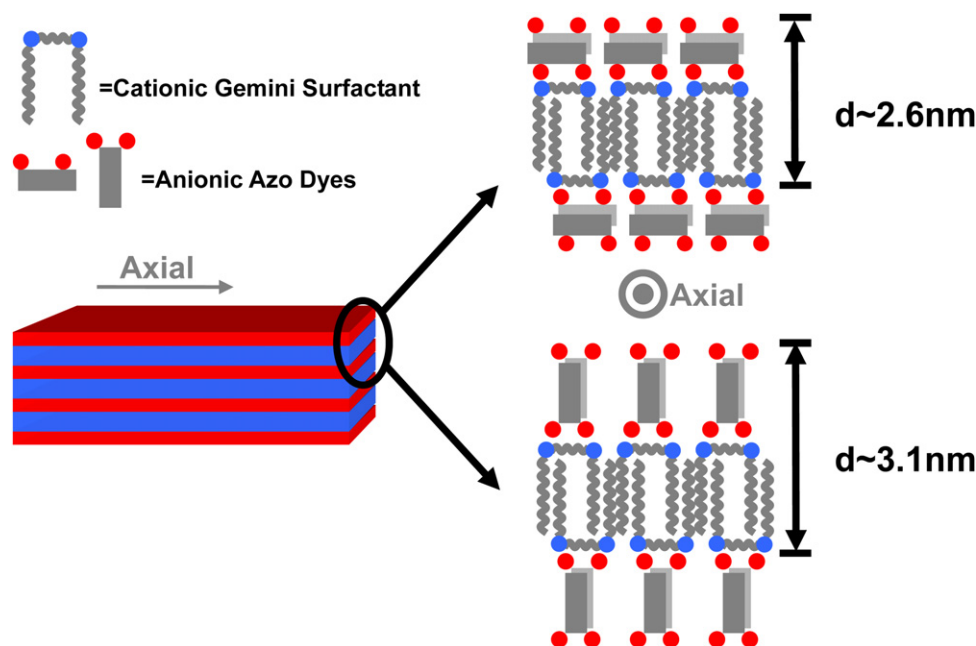


Fig. 7. Model for the possible structure of dye/surfactant assemblies.

Table 3
The aggregation states of azo dyes/surfactants with different size of the head groups.

surfactant	AR	AR13	BR
DDHC	nano-fibers (Fig. 9e)	nano-fibers (Fig. 9f)	nano-fibers (Fig. 9g)
DTAB	nano-fibers (Fig. 9a)	nano-fibers (Fig. 9d)	plate-like
DEAB	vesicle (Fig. 8b)	vesicle	vesicle
DPAB	vesicle (Fig. 8d)	vesicle	vesicle
DPyB	plate-like	plate-like	plate-like
DMIImB	plate-like	plate-like	plate-like

ones such as triethyl or tripropyl groups, the mixtures become clear solutions. TEM and DLS results reveal that the assemblies are fragments with an average hydrodynamic radius of 20 nm and vesicles 50–200 nm. (Fig. 8) This may be attributed to the stereo effect aroused by the larger surfactant heads which leads to a smaller packing parameter [41]. Therefore, the curvature of the self-assembled structures increases so that 1-D nano-structures are disfavored.

The 1-D structure formation was closely related with the subtle stacking of the conjugated groups of the dyes in the above mixed systems. For instance, if the packing was disturbed by using surfactants with bulky aromatic groups, such as dodecylpyridinium bromide (DPyB) and dodecylmethylimidazolium bromide (DMIImB), only sheet-like structures were observed, suggesting that the aromatic head groups have disturbed the 1-D directional packing of the dyes.

It is well-known that hydrophobic effect will be greatly influenced by the surfactant chain length. In order to study this effect on the formation of 1-D structures, cationic surfactants with different

hydrocarbon chain length were selected and studied in the mixed systems of azo dyes and cationic surfactants. (Table 4)

It is found in Table 4 that at the surfactant chain length being shorter, such as using OTAB, 1-D structures cannot be formed no matter with which dye. The assemblies in these systems are plate-like or short ribbons, and most of them are larger than 1 μm both in width and length. When the carbon number of the surfactant chains reached 12, nano-fibers are formed in the AR and AR13 systems (Fig. 9a and d). However, with the hydrocarbon chain of the surfactants being longer, the assemblies become shorter with the width beyond five hundreds nanometers and length over micrometers. Similar situations also occurred in Gemini surfactants systems. XRD results (Fig. 10) demonstrate that when the hydrophobic chains are shortened to 8C, the peak of pure AR crystal shows up instead the peak of AR/surfactant complex. When the chain grows longer to 10C, the peak of AR/surfactant complex occurs, but the peak of pure AR is still there. As the chain was extended to 12C, the peak of pure AR disappears. With further increasing of the chain lengths, the peak of AR/surfactant remains, and the aggregates grows larger. These phenomena suggest that only appropriate hydrophobic effect is beneficial to the 1-D nano-structure formation. If the hydrophobic chains are too short, the hydrophobic effect is not strong enough to form AR/surfactant complex. On the contrary, as the hydrophobic chains become too long, the hydrophobic effect is too strong, and the aggregates tend to grow into bigger ones with larger aggregation number to decrease the chains' contact area with water. Only when the hydrophobic chains have a length of 12C, the hydrophobic effect is suitable to form nano-fibers.

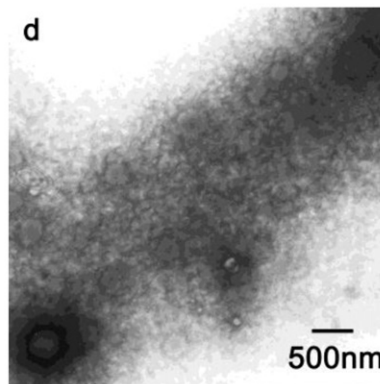
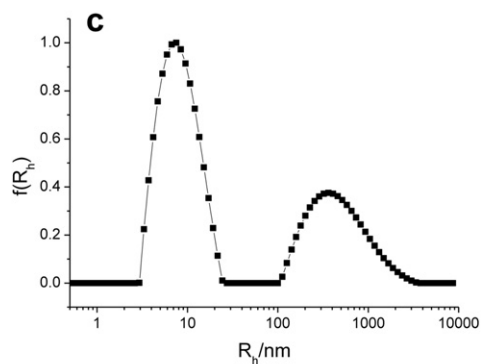
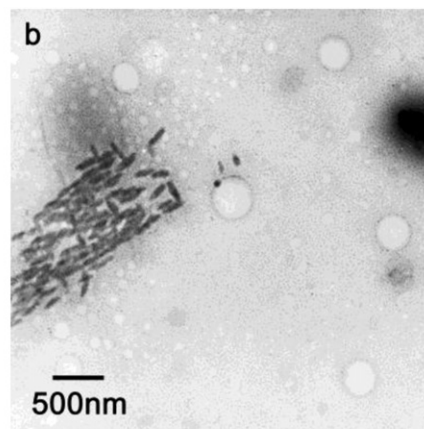
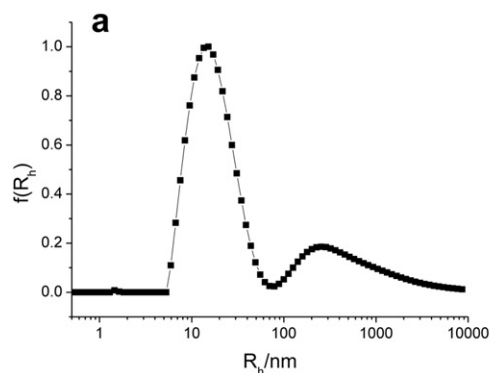


Fig. 8. (a) Size distribution and (b) TEM image of AR/DEAB charge ratio = 1:1 $C_T = 1$ mM system; (c) Size distribution and (d) TEM image of AR/DPAB charge ratio = 1:1 $C_T = 1$ mM system.

Table 4
The assemblies of azo dyes/surfactants with different hydrocarbon chains length.

surfactant	AR	AR13	BR
OTAB	plate-like (Fig. 9c)	short ribbon	plate-like
DeTAB	plate-like	short ribbon	rodlike
DTAB	nano-fibers (Fig. 9a)	nano-fibers (Fig. 9d)	short ribbon
TTAB	plate-like ribbon and nano-fibers (Fig. 9b)	plate-like nano-fibers and ribbon	short ribbon
CTAB	plate-like	plate-like	ribbon
8-6-8(Me)	plate-like	nano-fibers (Fig. 2d)	plate-like
12-6-12(Me)	nano-helices (Fig. 2g)	nano-fibers (Fig. 2d)	nano-fibers (Fig. 2f)
16-6-16(Me)	ribbon	ribbon	ribbon

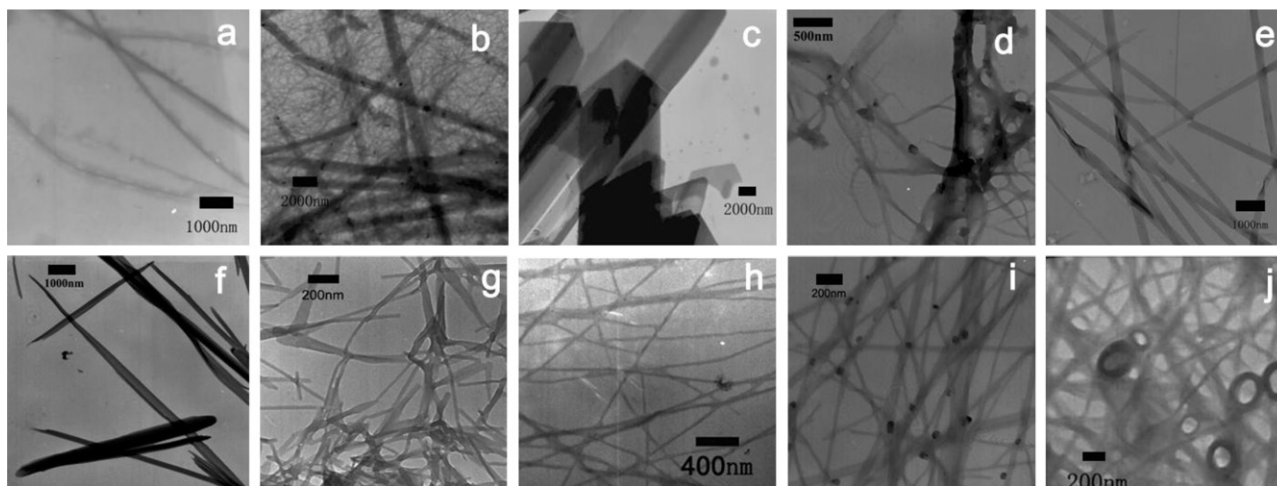


Fig. 9. TEM image of (a) AR/DTAB charge ratio = 1:1 $C_T = 1$ mM; (b) AR/CTAB charge ratio = 1:1 $C_T = 1$ mM; (c) AR/OTAB charge ratio = 1:1 $C_T = 1$ mM; (d) AR13/DTAB charge ratio = 1:1 $C_T = 1$ mM; (e) AR/ $C_{12}NH_3Cl$ charge ratio = 1:1 $C_T = 1$ mM; (f) AR13/ $C_{12}NH_3Cl$ charge ratio = 1:1 $C_T = 1$ mM; (g) BR/DDHC charge ratio = 2:1 $C_T = 1$ mM; (h) AR/12-10-12(Me) 1:1 $C_T = 1$ mM; (i) AR13/12-10-12(Me) 1:1 $C_T = 1$ mM; (j) BR/12-10-12(Me) 2:1 $C_T = 1$ mM.

Table 5
The aggregation states of azo dyes/Gemini surfactants with different spacer lengths.

surfactant	AR	AR13	BR
12-2-12(Me)	plate-like	plate-like	plate-like
12-4-12(Me)	plate-like	plate-like	plate-like
12-6-12(Me)	nano-fibers and nano-helices (Fig. 2g)	nano-fibers (Fig. 2d)	nano-fibers (Fig. 2f)
12-10-12(Me)	nano-fibers (Fig. 9h)	nano-fibers (Fig. 9i)	nano-fibers (Fig. 9j)

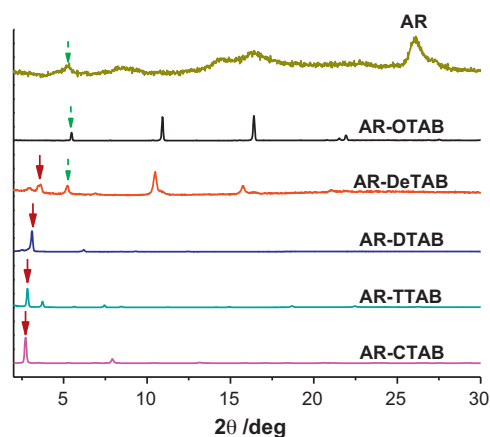


Fig. 10. X-Ray Diffraction of the complexes of AR and cationic surfactants with different length of hydrophobic chains.

In case of the employment of Gemini surfactants, the spacer length of the Gemini surfactants is also crucial on the morphology of the aggregates. (Table 5) When the carbon number of the spacer is 2 or 4, it tends to form sheet-like structures in the mixed systems. Only at the carbon number of the spacer being 6 or 10, 1-D nano-fibers can be formed. It seems that the spacer length play a similar role as the hydrocarbon chains of the surfactant which is to increase the hydrophobic effect.

4. Conclusions

In conclusion, 1-D nano-structures can be constructed from the mixed systems of azo dyes and cationic surfactants in a broad range of concentration and mixing ratio. The formation of 1-D nano-structures can be regulated from the molecular level, such as variation of the conjugated groups of the dyes, change of the head group size and the chain length of cationic surfactants. Our study suggests that 1-D assembly formation is controlled by multiple interactions in these systems. Electrostatic attraction, hydrophobic effect, and geometric packing all influence the morphology of the 1-D assemblies. The results in this work are instructive to further understanding and controlling of the assembly of 1-D nano-structures.

Acknowledgments

This research was supported by National Natural Science Foundation of China (50821061 and 21073006) and Doctorial Fund of Ministry of Education of China.

References

- [1] X.F. Duan, Y. Huang, Y. Cui, J.F. Wang, C.M. Lieber, Indium phosphide nanowires as building blocks for nanoscale electronic and optoelectronic devices, *Nature* 409 (2001) 66–69.
- [2] Y. Huang, X.F. Duan, Y. Cui, L.J. Lauhon, K.H. Kim, C.M. Lieber, Logic gates and computation from assembled nanowire building blocks, *Science* 294 (2001) 1313–1317.
- [3] D.H. Cobden, Molecular electronics – nanowires begin to shine, *Nature* 409 (2001) 32–33.
- [4] R.F. Service, Assembling nanocircuits from the bottom up, *Science* 293 (2001) 782–785.
- [5] P.M. Rorvik, T. Grande, M.A. Einarsrud, One-dimensional nanostructures of ferroelectric perovskites, *Adv. Mater.* 23 (2011) 4007–4034.
- [6] M. Yu, Y.Z. Long, B. Sun, Z.Y. Fan, Recent advances in solar cells based on one-dimensional nanostructure arrays, *Nanoscale* 4 (2012) 2783–2796.
- [7] J.F. Wang, M.S. Gudiksen, X.F. Duan, Y. Cui, C.M. Lieber, Highly polarized photoluminescence and photodetection from single indium phosphide nanowires, *Science* 293 (2001) 1455–1457.
- [8] M.H. Huang, S. Mao, H. Feick, H.Q. Yan, Y.Y. Wu, H. Kind, E. Weber, R. Russo, P.D. Yang, Room-temperature ultraviolet nanowire nanolasers, *Science* 292 (2001) 1897–1899.
- [9] Y.N. Xia, P.D. Yang, Y.G. Sun, Y.Y. Wu, B. Mayers, B. Gates, Y.D. Yin, F. Kim, Y.Q. Yan, One-dimensional nanostructures: synthesis, characterization, and applications, *Adv. Mater.* 15 (2003) 353–389.
- [10] C.Z. Li, H.X. He, A. Bogozzi, J.S. Bunch, N.J. Tao, Molecular detection based on conductance quantization of nanowires, *Appl. Phys. Lett.* 76 (2000) 1333–1335.
- [11] E.C. Walter, F. Favier, R.M. Penner, Palladium mesowire arrays for fast hydrogen sensors and hydrogen-actuated switches, *Anal. Chem.* 74 (2002) 1546–1553.
- [12] Y. Cui, Q.Q. Wei, H.K. Park, C.M. Lieber, Nanowire nanosensors for highly sensitive and selective detection of biological and chemical species, *Science* 293 (2001) 1289–1292.
- [13] S. Chattopadhyay, L.C. Chen, K.H. Chen, Energy production and conversion applications of one-dimensional semiconductor nanostructures, *NPG Asia Mater.* 3 (2011) 74–81.
- [14] T. Scheibel, Protein fibers as performance proteins: new technologies and applications, *Curr. Opin. Biotechnol.* 16 (2005) 427–433.
- [15] W.H. Binder, O.W. Smrzka, Self-assembly of fibers and fibrils, *Angew. Chem. Int. Ed.* 45 (2006) 7324–7328.
- [16] C.A. Ross, M.A. Poirier, Protein aggregation and neurodegenerative disease, *Nat. Med.* 10 (2004) S10–S17.
- [17] O.S. Makin, E. Atkins, P. Sikorski, J. Johansson, L.C. Serpell, Molecular basis for amyloid fibril formation and stability, *PNAS* 102 (2005) 315–320.
- [18] J.P. Guo, T. Arai, J. Miklosy, P.L. McGeer, A beta and tau form soluble complexes that may promote self aggregation of both into the insoluble forms observed in Alzheimer's disease, *PNAS* 103 (2006) 1953–1958.
- [19] A.P. Alivisatos, Semiconductor clusters, nanocrystals, and quantum dots, *Science* 271 (1996) 933–937.
- [20] T.J. Trentler, K.M. Hickman, S.C. Goel, A.M. Viano, P.C. Gibbons, W.E. Buhro, Solution-liquid-solid growth of crystalline III-V semiconductors – an analogy to vapor-liquid-solid growth, *Science* 270 (1995) 1791–1794.
- [21] J.H. Jung, H. Kobayashi, K.J.C. van Bommel, S. Shinkai, T. Shimizu, Creation of novel helical ribbon and double-layered nanotube TiO₂ structures using an organogel template, *Chem. Mater.* 14 (2002) 1445–1447.
- [22] S. Kobayashi, N. Hamasaki, M. Suzuki, M. Kimura, H. Shirai, K. Hanabusa, Preparation of helical transition-metal oxide tubes using organogelators as structure-directing agents, *J. Am. Chem. Soc.* 124 (2002) 6550–6551.
- [23] E.D. Sone, E.R. Zubarev, S.I. Stupp, Semiconductor nanohelices templated by supramolecular ribbons, *Angew. Chem. Int. Ed.* 71 (2002), 1705.
- [24] A.M. Seddon, H.M. Patel, S.L. Burkett, S. Mann, Chiral templating of silica-lipid lamellar mesophase with helical tubular architecture, *Angew. Chem. Int. Ed.* 41 (2002) 2988–2991.
- [25] J.H. Jung, H. Kobayashi, M. Masuda, T. Shimizu, S. Shinkai, Helical ribbon aggregate composed of a crown-appended cholesterol derivative which acts as an amphiphilic gelator of organic solvents and as a template for chiral silica transcription, *J. Am. Chem. Soc.* 123 (2001) 8785–8789.
- [26] Y.Y. Lin, Y. Qiao, X.H. Cheng, Y. Yan, Z.B. Li, J.B. Huang, Hydrotropic salt promotes anionic surfactant self-assembly into vesicles and ultralong fibers, *J. Colloid Interface Sci.* 369 (2012) 238–244.
- [27] Y.Y. Lin, Y. Qiao, P.F. Tang, Z.B. Li, J.B. Huang, Controllable self-assembled laminated nanoribbons from dipeptide-amphiphile bearing azobenzene moiety, *Soft Matter* 7 (2011) 2762–2769.
- [28] Y.Y. Lin, A.D. Wang, Y. Qiao, C. Gao, M. Drechsler, J.P. Ye, Y. Yan, J.B. Huang, Rationally designed helical nanofibers via multiple non-covalent interactions: fabrication and modulation, *Soft Matter* 6 (2010) 2031–2036.
- [29] Y. Qiao, Y.Y. Lin, Z.Y. Yang, H.F. Chen, S.F. Zhang, Y. Yan, J.B. Huang, Unique temperature-dependent supramolecular self-assembly: from hierarchical 1D nanostructures to super hydrogel, *J. Phys. Chem. B* 114 (2010) 11725–11730.
- [30] Y. Qiao, Y.Y. Lin, Y.J. Wang, Z.Y. Yang, J. Liu, J. Zhou, Y. Yan, J.B. Huang, Metal-driven hierarchical self-assembled one-dimensional nanohelices, *Nano Lett.* 9 (2009) 4500–4504.
- [31] Y. Yan, Y.Y. Lin, Y. Qiao, J.B. Huang, Construction and application of tunable one-dimensional soft supramolecular assemblies, *Soft Matter* 7 (2011) 6385–6398.
- [32] Z.C. Wang, C.J. Medforth, J.A. Shelnutt, Porphyrin nanotubes by ionic self-assembly, *J. Am. Chem. Soc.* 126 (2004) 15954–15955.
- [33] Y. Guan, S.H. Yu, M. Antonietti, C. Bottcher, C.F.J. Faul, Synthesis of supramolecular polymers by ionic self-assembly of oppositely charged dyes, *Chem. Eur. J.* 11 (2005) 1305–1311.
- [34] G.H. Fu, M.L. Wang, Y.L. Wang, N. Xia, X.J. Zhang, M. Yang, P. Zheng, W. Wang, C. Burger, Ionic self-assembled derivatives of perylene-tetracarboxylic dianhydride: facile synthesis, morphology and structures, *New J. Chem.* 33 (2009) 784–792.
- [35] D. Graebner, L. Zhai, Y. Talmon, J. Schmidt, N. Freiberger, O. Glatter, B. Herzog, H. Hoffmann, Phase behavior of aqueous mixtures of 2-phenylbenzimidazole-5-sulfonic acid and cetyltrimethylammonium bromide: hydrogels, vesicles, tubules, and ribbons, *J. Phys. Chem. B* 112 (2008) 2901–2908.
- [36] F. Camerel, C.F.J. Faul, Combination of ionic self-assembly and hydrogen bonding as a tool for the synthesis of liquid-crystalline materials and organogelators from a simple building block, *Chem. Commun.* (2003) 1958–1959.
- [37] F. Camerel, P. Strauch, M. Antonietti, C.F.J. Faul, Copper-metallomesogen structures obtained by ionic self-assembly (ISA): molecular electromechanical switching driven by cooperativity, *Chem. Eur. J.* 9 (2003) 3764–3771.
- [38] Y.W. Huang, Y. Yan, B.M. Smarsly, Z.X. Wei, C.F.J. Faul, Helical supramolecular aggregates, mesoscopic organization and nanofibers of a perylenebisimide-chiral surfactant complex via ionic self-assembly, *J. Mater. Chem.* 19 (2009) 2356–2362.
- [39] T. Lu, F. Han, G.R. Mao, G.F. Lin, J.B. Huang, X. Huang, Y.L. Wang, H.L. Fu, Effect of hydrocarbon parts of the polar headgroup on surfactant aggregates in gemini and bola surfactant solutions, *Langmuir* 23 (2007) 2932–2936.
- [40] Y. Guan, M. Antonietti, C.F.J. Faul, Ionic self-assembly of dye-surfactant complexes: influence of tail lengths and dye architecture on the phase morphology, *Langmuir* 18 (2002) 5939–5945.
- [41] J.N. Israelachvili, D.J. Mitchell, B.W. Ninham, Theory of self-assembly of hydrocarbon amphiphiles into micelles and bilayers, *J. Chem. Soc., Faraday Trans. II* 72 (1976) 1525–1568.